Machine Learning (ML)-Based Prediction and Compensation of Springback for Tube Bending

J. Ma, H. Li, G. Y. Chen, T. Welo, and G. J. Li

Abstract Bent tubes are extensively used in the manufacturing industry to meet demands for lightweight and high performance. As one of the most significant behaviors affecting the dimensional accuracy in tube bending, springback causes problems in tube assembly and service, making the manufacturing process complex, time-consuming, and difficult to control. This paper attempts to present an accurate, efficient, and flexible strategy to control springback based on Machine Learning (ML) modeling. An enhanced PSO-BP network-based ML model is established, providing a strong ability to account for the influences of material, geometry, and process parameters on springback. For supervised learning, training sample data can be collected from the historical production process or, alternatively, finite element simulation and laboratory-type experiments. Using the cold bending of aluminum tubes as the application case, the ML model is evaluated with high reliability and efficiency in springback prediction and compensation strategy of springback.

Keywords Springback · Tube bending · Machine learning · Compensation

J. Ma · H. Li (✉) · G. Y. Chen
State Key Lab of Solidification Processing, School of Materials Science and Engineering, Northwestern Polytechnical University, Xi'an 710071, China
e-mail: liheng@nwpu.edu.cn

J. Ma
e-mail: jun.ma@ntnu.no

J. Ma · T. Welo
Department of Mechanical and Industrial Engineering, Norwegian University of Science and Technology, Trondheim 7491, Norway

G. J. Li
Chengdu Aircraft Industry (Group) Co., Ltd, Chengdu 610092, China

G. Daehn et al. (eds.), *Forming the Future*, The Minerals, Metals & Materials Series,
https://doi.org/10.1007/978-3-030-75381-8_13

1 Introduction

As one of the crucial structures for mass/heat transferring and load bearing with enormous quantities and diversities, bent tubular parts have attracted increased application in most industrial fields, such as automobile, aerospace, energy, and so on [1–3]. Springback is a significant issue for tube bending. It refers to the changes of both angles and curvatures after removing the applied tools, leading to a series of problems such as increased tolerance limit, variabilities in assemble, and, sometimes, service performance [3, 4]. From the point of the manufacturing system, springback makes the forming process complex, significantly affecting the process flexibility [5] as well as the adaptive design of control strategies [6]. In addition, this critical problem becomes more dramatic in the manufacturing of complex 3D structures, as well as small production batches with diverse bending angles and curvatures [7]. Thus, achieving accurate control of springback is of importance to high-precision products and integrated design of smart manufacturing systems. However, springback is the "closing work" in a forming process, meaning that all possible factors from the aspects of material property, geometry, and processing conditions can make an impact on springback, thus making it difficult to control dimensional accuracy in tube bending.

Accurate prediction is the premise to achieve effective control of springback. In the past decades, analytical, experimental, and numerical methods have been widely used to estimate springback in metal forming [3, 4]. The analytical method allows fast springback calculation for simple forming cases, offering an advanced understanding of springback characteristics and mechanisms. The finite element (FE) numerical approach can simulate the actual forming process, in particular, with modeling of the complex contact/friction conditions and nonlinear material properties, thus providing accurate predictions of forming defects, such as thinning, distortion as well as springback once high reliability can be ensured. FE-assisted optimization of tooling and process parameters is widely used in the design stage of the forming process. The experimental approach, however, is generally based on "trial-and-error" to search for a satisfactory result. Furthermore, in recent years, several Deep Learning (DL) methods also emerge in springback analysis to explore the control of dimensional accuracy [8–10].

To this date, most FE-based works and DL-based attempts on springback are focused on sheet metal forming, yet with much less concern on the tube bending processes. The "trial-and-error" approach still acts as the main strategy for springback compensation in tube bending production [1, 3], in which at least 2–3 times bending trials are commonly needed to find out an acceptable compensation solution. It causes some critical problems, including production downtime, high costs, waste of materials, scrap, and increased process uncertainties. This is particularly true for the industrial production of bent tubular parts with small batches and multiple part configurations. Even though FE simulation can be used as the virtual "trial-and-error" to reduce the physical trials, it is also a non-added value operation to simulate all the possible forming conditions. In addition, FE simulation with the deterministic target

springback problem can hardly meet the need for process flexibility. To address these problems, it is a need to develop a feasible and effective strategy that can provide a reliable and fast evaluation of compensation for springback, at the same time, with the possibility for the integrated design of closed-loop-control to improve the product accuracy and enhance the process flexibility for tube bending.

To this aim, this work attempts to develop a flexible strategy for springback prediction and compensation in tube bending based on the ML modeling framework. Training datasets for supervised learning can come from the historical production process, alternatively laboratory-type experiments, and FE simulation. Using the cold bending of aluminum alloy (Al-alloy) tubes as the application case, the ML model is verified in both springback prediction and compensation. Based on this research, an outlook on the future development and industrial application of the ML-based springback control strategy is presented.

2 Methodology

2.1 Overview of ML-Based Modeling for Springback

As mentioned above, almost all the possible factors throughout the forming process can make a difference in springback. In fact, as shown in Fig. 1, in addition to springback, the other geometry dimensions, such as wall thickness, ovalization, etc., as well as product performance, such as working pressure, fatigue, etc., are closely related to the above-mentioned influential factors from the aspect of material, geometry, and process. To this end, a "bridge" can be built to link the various input and/or in-process

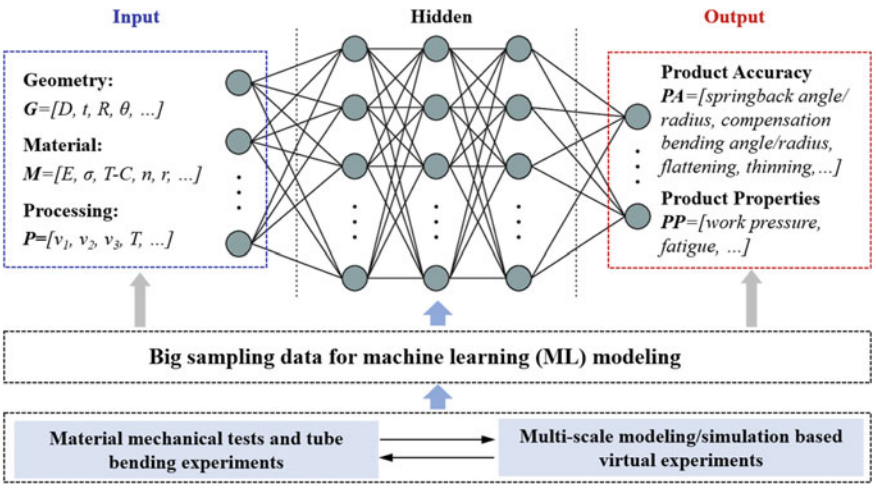

Fig. 1 Overview of the ML-based modeling for tube bending

variables and different output indexes based on big-data mining and analysis, thus achieving better control of product quality and forming process, as well as reducing the manufacturing investment.

However, the accuracy and reliability of the "bridge" model highly depend on the number and quality of sampling data. If the data is all from physical experiments, it will uncourtly cause dramatic time consumption and high cost, especially in small production batches with diverse angles, radius, and spatial structures. Therefore, the idea of this model is to establish the sampling data source by combining typical experiments, such as material property tests and forming experiments, and the multi-scale simulation-based virtual experiments, such as through-process FE simulation of bending–springback. Based on the big-data analysis, a machine learning model can be constructed to map the relation between multiple input variables and springback, thus achieving accurate compensation for springback in tube bending.

2.2 *Rotary Draw Bending and Springback*

Rotary draw bending (RDB) is taken as the forming process in the application. RDB is the most commonly used method for the manufacturing of bent tubes with high dimension accuracy. As shown in Fig. 2a, the whole tube is subjected to the multi-tool constraints; viz., bend die, clamp die, pressure die, wiper die, and flexible mandrel die. Under the joint action of a multi-tool, the tube is drawn around the bending center to form a bent tube with a certain bending radius and angle. Then, the tube is unloaded upon removal of the tools, and springback occurs, as shown in Fig. 2b. Springback in tube bending can cause both changes of released bending angle and radius. For a targeted bending geometry, the processing conditions are always pre-determined after optimization.

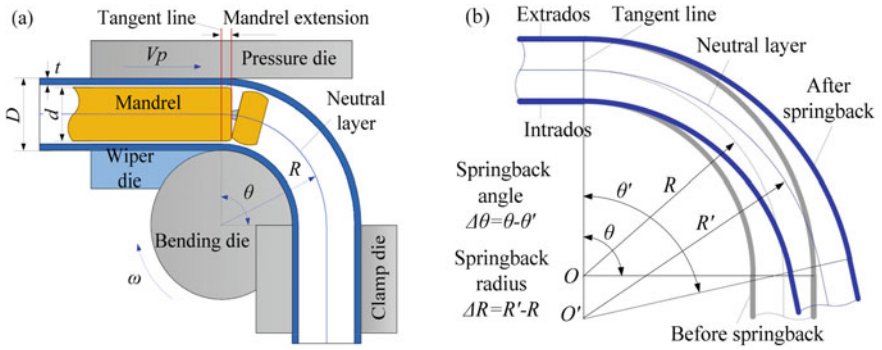

Fig. 2 Schematic view of rotary draw bending: **a** forming principle and tooling system; **b** unloading springback. (Color figure online)

In order to characterize the springback under different bending angles, a springback ratio coefficient is defined as follows:

$$\eta = \Delta\theta \big/ \theta_b = (\theta_b - \theta_a) \big/ \theta_b \tag{1}$$

where η is the springback ratio coefficient, $\Delta\theta$ denotes the amount of springback angle, θ_b and θ_a represent the bending angle before unloading and actual angle after springback, respectively.

As for springback compensation, a compensation coefficient is also defined as shown in Eq (2):

$$C = \Delta\theta_c \big/ \theta_t = (\theta_c - \theta_t) \big/ \theta_t \tag{2}$$

where C is the compensation coefficient, θ_t is the targeted bending angle, and $\Delta\theta_c$ is the amount of compensation angle. Here, θ_c is the compensated bending angle, which can further be calculated as follows:

$$\theta_c = (1 + C)\theta_t \tag{3}$$

If the compensation coefficient can be identified, the springback compensation thus can be realized. However, achieving this coefficient presumes an accurate prediction of the springback angle under different bending conditions.

3 Machine Learning Modeling

A myriad of ML algorithms has been developed to address the problems with different features. Among these algorithms, the backpropagation (BP) neural network is the most widely used due to its advanced algorithm structure, which shows a strong ability and potential in recognizing the underlying complicated patterns in engineering tasks [11]. Furthermore, there is a number of successful experiences with utilizing the BP neural network in manufacturing processes, such as stamping, additive manufacturing [12]. Therefore, in this work, the BP neural network is employed as the base to model the relationship between the input variables and springback for tube bending process.

3.1 BP Neural Network

The BP neural network is a multi-layer feedforward network algorithm that is trained according to an error backpropagation scheme [13]. A three-layer BP network with the input layer, the hidden layer, and the output layer is selected as the baseline to construct the ML model. The Hecht–Nelson method is used to determine the node

number of the hidden layer; that is, the node number of the hidden layer is (2n + 1) times the node number of the input layer. For the output, only the springback ratio or compensation coefficient is the objective in this work, which implies that the node number is just set as one.

The basic procedure of the BP network is described as follows:

Step 1: Calculation of hidden layer output:

$$H_j = f\left(\sum_{i=1}^{n} w_{j,i} \cdot x_i + a_j\right) \tag{4}$$

where $w_{j,i}$ represents the connection weight from input node i to hidden node j, a_j is the bias of the neuron j, H_j is the output of hidden layer node j, and f is the activation function of a node.

Step 2: Calculation of the final output:

$$O_k = f_{\mathrm{o}}\left(\sum_{k=1}^{m} w_{k,j} \cdot H_j + b_k\right) \tag{5}$$

where $w_{k,j}$ represents the connection weight from hidden node j to output node k, b_k is the bias of the neuron k, O_k is the output data, and f_{o} is the activation function of output layer nodes.

Step 3: Global minimization of error by training the algorithm:

$$e_k = \sum_{k=1}^{m} |y_k - O_k| \tag{6}$$

where e_k is the error and y_k represents the experimental result of output node k.

Step 4: Check of error tolerance and update of weight coefficients.

3.2 PSO Algorithm

Particle swarm optimization (PSO) was proposed by Kennedy and Eberhart [14], representing an evolutionary computation algorithm inspired by the flocking behavior. In the PSO algorithm, a swarm of particles keeps moving around in a problem space according to the best-known positions of each particle and the entitle swarm, in searching for the optimal solution. The position and moving velocity of the particles in the D-dimensional space are described as follows:

$$\begin{cases} V_i^{t+1} = w^t V_i^t + c_1 r_1 \left(p_{\mathrm{best},i}^t - X_i^t\right) + c_2 r_2 \left(g_{\mathrm{best},i}^t - X_i^t\right) \\ X_i^{t+1} = X_i^t + V_i^{t+1} \end{cases} \tag{7}$$

where X_i^t is the position of particle i in at the t^{th} iteration, V_i^t represents the velocity of this particle, c_1 and c_2 are the learning factors controlling how far a particle can move in a single iteration, and r_1 and r_2 are two random number within [0, 1]. In Eq. (7), $p_{\text{best},i}^t$ and $g_{\text{best},i}^t$ are the optimal position of the particle and the global optimal position of all particles at the tth iteration, respectively, and the w^t is the inertia weight coefficient that makes a balance of the local and global search ability.

In the PSO algorithm, the linearly decreasing inertia weight is commonly used. However, the linear decreasing weight has two drawbacks; viz., the low velocity of convergence when the best point can be detected at an early computation state, and the decreased global search ability with decreasing the weight [15]. Thus, in this model, a nonlinear inertia weight is used to improve the search ability, as shown in Eq. (8):

$$w^t = w_{\max} - \left(w_{\max} - w_{\min}\right) \cdot \tan\left(t \Big/ t_{\max} - \pi \Big/ 4\right) \tag{8}$$

where $w_{\max}$ and $w_{\min}$ are the maximum and minimum inertia weight, and $t_{\max}$ is the maximum iteration, respectively.

In addition, to further improve the global search ability of the PSO algorithm, a crossover operator can be applied after each iteration [16]. According to a given crossover probability, a certain number of particles will be chosen for random hybridization, and then the same number of offspring particles are generated. The position of the offspring particle is determined as

$$X^t = r X_I^t + (1 - r) X_{II}^t \tag{9}$$

where r is a random value within [0, 1], and the subscript "I" and "II" are two parent particles.

The velocity of the offspring particle is calculated by Eq. (10) from their parent particles.

$$V^t = \left|V_I^t\right|\left(V_I^t + V_{II}^t\right) \Big/ \left|V_I^t + V_{II}^t\right| \tag{10}$$

Through the crossover operator, the offspring particles can avoid falling into the local optimization, thus improving the global search ability.

3.3 Enhanced PSO-BP-Based ML Model

By combining the BP neural network and the PSO algorithm with a crossover operator, an enhanced PSO-BP-based machine learning model is thus established. Figure 3 demonstrates the computation flowchart of the proposed ML model. Based on Matlab, the model is numerically implemented for the application in the next section.

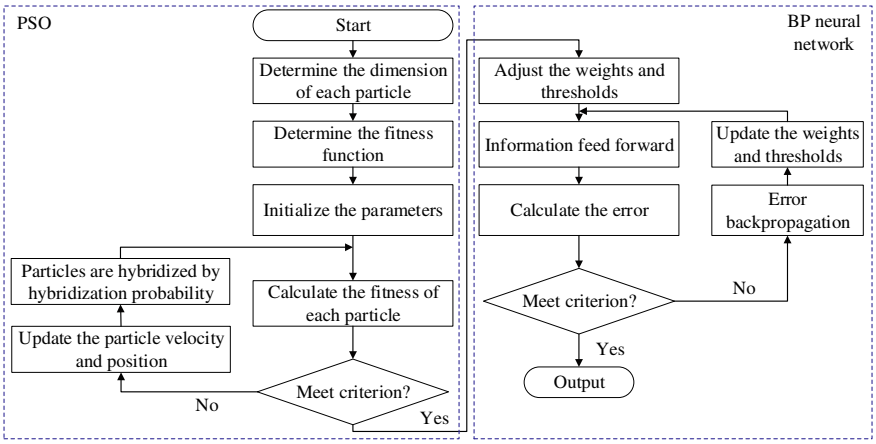

Fig. 3 Flowchart of the enhanced PSO-BP neural network model. (Color figure online)

4 Application and Evaluation

In this application, AA5052-O tubes with eight types of specifications (diameter and thickness) are used. Even though the material grades are the same, variations exist in the mechanical properties between different specifications. Table 1 shows the mechanical properties obtained by uniaxial tension tests, indicating a significant variation in the elastic modulus, yield strength, working hardening, etc. Springback magnitude is determined by the bending moments, elastic modulus, and residual stress after unloading, etc. All the mechanical parameters listed in Table 1 can cause an influence on the stress/strain distribution, further affecting the springback. Therefore, the above material parameters are set as the independent input variables in the ML model. Besides, the geometry parameters—viz., outer diameter, thickness, the

Table 1 Mechanical properties of Al-alloy tubes by uniaxial tension experiments

No.	Outer diameter [mm]	Thickness [mm]	Elastic modulus [MPa]	Yield strength [MPa]	Ultimate tensile strength [MPa]	Fraction elongation [%]	Working hardening exponent	*r*-value
#1	8	1	67244	45	216	22.48	0.328	0.500
#2	10	1	62485	81	220	16.09	0.315	0.929
#3	16	1	67428	70	250	28.57	0.286	0.858
#4	22	1	76190	67	247	25.66	0.302	0.924
#5	30	1	73267	43	180	27.11	0.316	0.628
#6	38	1	73642	81	300	24.14	0.341	0.599
#7	50	1.5	63368	31	128	24.98	0.330	0.635
#8	70	1.5	65671	47	182	26.17	0.346	0.486

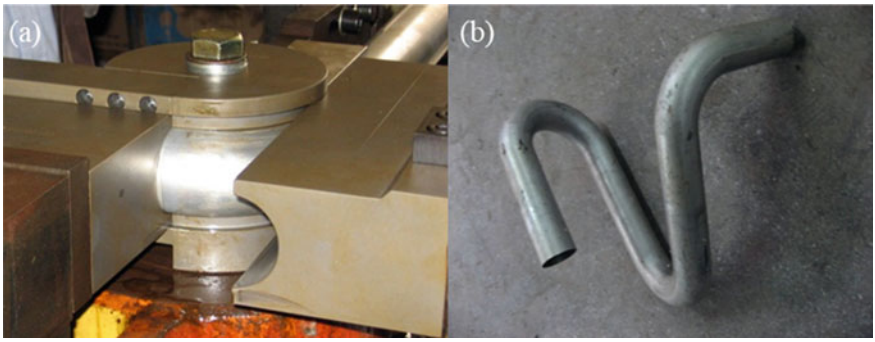

Fig. 4 Rotary draw bending experiment: **a** forming process; **b** Φ50 × t1.5 × 2D bent part. (Color figure online)

ratio of bending radius to outer diameter, and bending angle—are also set as independent input variables. As the tooling/process parameters are generally determined after optimization and then keep constant in production, these parameters are not considered in this work. Figure 4 shows the rotary draw bending process and the typical experimental part.

For the supervised machine learning of this model, the training sample set should be first established. In this application case, only the experimental data collected from the historical tube bending production in a company be used to establish the big-data source, and further to explore the feasibility of the ML model. The training sample data source is comprised of 46 sets of experimental input and springback data, which is acquired from the industrial production process in the company. The training set covers different bending geometries of the above-described eight types of tubular materials, in which the range of bending angle is $\theta = 9$~$122.2°$, and the range of relative bending radius is $R = 2$~$3D$. As shown in Table 2, five sets of experimental inputs are chosen as the test samples to evaluate the prediction accuracy. According to the description in Sect. 3, the parameters related to the ML model are determined

Table 2 Springback prediction based on the ML model

Input				Sp. prediction output + actual result			
D [mm]	t [mm]	Relative bending radius, R/D	Bending angle, θ_b [°]	Exp. sp. angle, $\Delta\theta_{exp}$ [°]	Pred. sp. angle, $\Delta\theta_{pred}$ [°]	Absolute error [°]	Relative error [%]
10	1.0	3	34.20	2.20	2.39	0.19	8.50
16	1.0	2	34.50	1.10	1.02	0.08	7.45
22	1.0	2	66.20	1.30	1.26	0.04	3.31
30	1.0	2	91.20	1.70	1.55	0.15	9.00
70	1.5	2	52.50	1.70	1.65	0.05	3.18

Table 3 Springback compensation based on the ML model

Input				Sp. compensation output + actual result			
D [mm]	t [mm]	Relative bending radius, R/D	Target bending angle, θ_t [°]	Exp. comp. angle, $\Delta\theta_{c,exp}$ [°]	Pred. comp. angle, $\Delta\theta_{c,pred}$ [°]	Absolute error [°]	Relative error [%]
10	1.0	3	32.00	2.20	2.11	0.09	3.91
16	1.0	2	33.40	1.10	0.81	0.29	26.10
22	1.0	2	64.90	1.30	1.21	0.09	7.08
30	1.0	2	89.50	1.70	1.91	0.21	12.53
70	1.5	2	50.80	1.70	1.65	0.05	2.82

as follows: the number of particles: 40, learning coefficient: 2.05, maximum weight: 0.9, minimum weight: 0.4, maximum velocity: 1, hybrid probability: 0.7.

After 34 iterations within 300 s, the prediction results can be calculated, as shown in Table 2. It can be found that the maximum absolute error is 0.188°, the average relative error is 6.29%. Compared with the traditional PSO-BP model, by introducing the crossover operator, not only the prediction accuracy is greatly improved but also the computation time is significantly reduced from 1.5 h to 300 s. For the springback compensation, the computation is completed after 32 iterations within 200 s. As shown in Table 3, the predicted compensation angles can agree with the experimental ones except for one abnormal case. The average absolute error and relative of the compensation angle are 0.15° and 10.49%, respectively. The maximum absolute error is 0.29°, which also meets the tolerance of $\pm$ 0.3° in many application cases.

However, we can find from the predictions of both springback angles and compensation angles, as shown in Tables 2 and 3, that there is still a pronounced variation in the prediction errors, which indicates a probability that an unacceptable prediction occurs. The reason for this variation might be attributed to the sample data used for training the ML model. In this application, the tube specifications (i.e., outer diameter and thickness), and bending geometries (i.e., bending angle and bending radius) vary significantly, however, training data only comprise 46 sets of experimental data from the historical production process. The accuracy of machine learning is sensitive to the number of samples and enlarging the high-quality datasets with a certain range can improve the performance [10, 17]. Thus, for the problem in this work, increasing the size of high-quality training datasets may be helpful to the improvement of springback prediction and compensation. However, it does not mean that the more data of samples, the better performance of the model. The large size of datasets always means an increased computation time. Besides, machine learning can show effectiveness when it is applied to limited types and size of data and well-defined tasks [10]. It needs further exploration to find an optimal size of datasets, thus ensuring the performance as well as balancing the efficiency of the ML model.

5 Conclusions and Outlook

This paper presents a Machine Learning framework for springback prediction and compensation in tube bending towards the improvement of product dimensional accuracy, and process flexibility. The model is based on an enhanced PSO-BP algorithm, which enables a strong ability to address the complex influences of material properties, bending geometries and process parameters on springback, at the same time, has a high computation efficiency. Using the cold rotary draw bending process of Al-alloy tubes, the ML model is verified with high accuracy and efficiency in both springback prediction and compensation. In this application case, the experimental data that are collected from the historical production process in a company is applied for model training. Both the flexible bending geometries (i.e., tube diameter, thickness, bending radius, and bending angle) and the variations of material properties (elastic modulus, yield strength, work hardening exponent, etc.) of the Al-alloy tubes with respect to different specifications are considered to accommodate their influences on springback. The process parameters, however, are not yet considered due to the limited real-time data collection in the forming process.

In future research work, FE simulation-based virtual experiments in combination with typical physical experiments will be used to provide a big-data source for supervised learning of the model, thus improving the prediction/compensation accuracy and reducing the manufacturing investment. In addition, the model will be integrated into the manufacturing system of tube bending, thus seeking a self-adaptive enhancement of the model capability by training with the real-time production data. Finally, a close-loop-control strategy of springback in tube bending will be explored based on the ML model with both offline and online learning.

Acknowledgments Financial assistance of the Commercial Aircraft Research & Development Project of China (MJ-2016-G-64), National Science Funds of China (51522509, 51775441) and NTNU Aluminum Product Innovation Center (NAPIC) is acknowledged.

References

1. Li H, Yang H, Ma J (2018) Tube bending forming technologies: advances and trends. In: Totten GE et al (eds) Encyclopedia of aluminum and its alloys. CRC Press, Boca Raton, pp 2732–2750
2. Li H Fu MW (2019) Deformation based processing of materials: behavior, performance, modeling, and control. Elsevier
3. Li H, Ma J, Liu BY et al (2018) An insight into neutral layer shifting in tube bending. Int J Mach Tools Manufac 126:51–70
4. Wagoner RH, Lim H, Lee MG (2013) Advanced issues in springback. Int J Plast 45:3–20
5. Yang DY, Bambach M, Cao J et al (2018) Flexibility in metal forming. CIRP Ann 67(2):743–765
6. Welo T (2012) Intelligent manufacturing systems: controlling elastic springback in bending. IFIP Int Conf Adv Prod Manag Syst, Rhodes, Greece, 24–26 Sept 2012
7. Allwood JM, Duncan SR, Cao J et al (2016) Closed-loop control of product properties in metal forming. CIRP Ann 65(2):573–596

8. Dezelak M, Pahole I, Ficko M et al (2012) Machine learning for the improvement of springback modelling. Adv Prod Eng Manag 1:17–26
9. Nasrollahi V, Arezoo B (2012) Prediction of springback in sheet metal components with holes on the bending area, using experiments, finite element and neural networks. Mater Des 36:331–336
10. Wang JJ, Ma YL, Zhang LB et al (2018) Deep learning for smart manufacturing: methods and applications. J Manuf Syst 48:144–156
11. Lecun Y, Bengio Y, Hinton G (2015) Deep learning. Nature 521(7553):436–444
12. Qi X, Chen G, Li Y et al (2019) Applying neural-network-based machine learning to additive manufacturing: current applications, challenges, and future perspectives. Engineering 5(4):721–729
13. Li J et al (2012) Brief introduction of backpropagation (BP) neural network algorithm and its improvement. Adv Comput Sci Inf Eng, Zhengzhou, China, 19–20 May 2012
14. Kennedy J, Eberhart, R (1995) Particle swarm optimization (PSO). IEEE Int Conf Neural Networks, Perth, Australia, 27 Nov–1 Dec 1995
15. Bansal JC et al (2011) Inertia weight strategies in particle swarm optimization. IEEE 3rd World Cong Nature Biol Inspir Comp, Salamanca, Spain, 19–21 Oct 2011
16. Chen Y, Li L, Xiao J et al (2018) Particle swarm optimizer with crossover operation. Eng Appl Artif Intel 70:159–169
17. Zhang Y, Ling C (2018) A strategy to apply machine learning to small datasets in materials science. Comput Mater 4(1):1–8